2018

Experimental Investigations Of Air-Cooler Operating Under Frost Conditions

Jerzy Gagan
Bialystok Technical University, Wiejska 45C, Bialystok, 15-351, Poland, j.gagan@pb.edu.pl

Kamil Smierciew
Bialystok Technical University, Wiejska 45C, Bialystok, 15-351, Poland, k.smierciew@pb.edu.pl

Dariusz Butrymowicz
Bialystok Technical University, Wiejska 45C, Bialystok, 15-351, Poland, d.butrymowicz@pb.edu.pl

Paweł Jakończuk
Bartosz, sp.j.,Sejneńska 7, 15399 Białystok, Poland, pjakonczuk@gmail.com

Experimental investigations of air-cooler operating under frost conditions

Jerzy GAGAN*[1], Kamil ŚMIERCIEW[1], Dariusz BUTRYMOWICZ[1], Paweł JAKOŃCZUK[1,2]

[1] Bialystok Technical University,
Wiejska 45C, Bialystok, 15-351, Poland
k.smierciew@pb.edu.pl

[2]Bartosz, sp.j., Sejneńska 7, 15-399 Białystok, Poland

* Corresponding Author

ABSTRACT

The fin-and-tube heat exchangers are extensively used in many fields, especially in HVACR (heat, ventilation, air-conditioning and refrigeration systems). When such heat exchangers operate as an air-coolers, in most of the cases, lower air temperature is achieved. When moist air flows across cold surfaces of the heat exchanger whose temperature is lower than the freezing point then frost formation will occur. This frost accumulation is undesirable in most cases since it negatively affects heat transfer due to the insulation of frost layer and causes pressure loss by blockage of air flow as the frost grows. This will lead to an undesirable degradation of the heat exchanger thermal performance. The analysis of the effect of the frosting process on the finned tube air cooler performance is presented in the paper. On the basis of the long-term experimental investigations of the air-cooler applied in the cold storage chamber the thermal degradation of the heat exchanger performance is discussed. The influence of the frost on the cooling capacity, by-pass factor and thermal resistance are shown. Temperature distribution of air passing through the air-cooler before and after the defrost procedure are presented and discussed. A method of the assessment of the amount of frost formed on the heat exchanger surface based on visualization of the cooler surface during operation and synchronized with the thermal measurements was developed. Analysis carried out with application of the proposed approach revealed that frosting causes deterioration of the tested air cooler refrigeration capacity up to 40%.

1. INTRODUCTION

Frosting, that occurs in many types of heat exchangers is an undesirable phenomenon as the layer of frost acts as an additional thermal resistance and decreases efficiency of heat transfer (Chiwon et al. 2017, Wu et al., 2016). Frost formation is a complex process, so its complex recognition as well as understanding of the degradation of heat transfer caused by frosting process may be still thought as an open research problem.

Various types of defrosting systems are used to remove frost from the surfaces of the heat exchangers (Reindl and Jekel, 2009, Song et al. 2018). Frequency of the defrosting process affects both energy efficiency of the cooling system and stored goods in the cold storage chamber. This is particularly important in the cold storage rooms where precise control of air parameters is often necessary.
It is easier to optimize the operation of the defrosting systems if the details of the frosting process are known. The paper presents an own approach of identification of the amount of frost on a heat exchanger surface. The proposed approach is based on the visualization of tested heat exchanger carried out during its operation. The method was validated using photos and thermal measurements taken during tests of an air cooler placed in a vegetables cold storage chamber.

2. DESCRIPTION OF PROPOSED METHODOLOGY

The locations of the sensors are shown in Fig. 1. The following measurements were made during the tests:

- relative humidity (RH) ; velocity (w), and temperature (T) of the outlet air;
- temperature (T) of the inlet air;
- inlet and outlet temperature (T) of glycol;
- temperature of the fins.
-

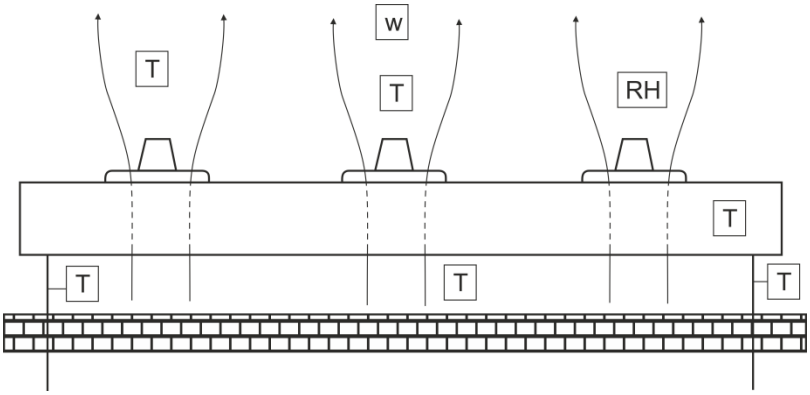

Figure 1: Sensor location diagram

The defrosting process lasted 10 minutes and was conducted two times a day. During defrosting air parameters in the tested cold storage chamber were changing rapidly affecting the storage conditions in various ways.

The amount of frost development on the cooler operation was determined by analysis of the photos taken with each measurement and saved as video files. Frosting process may be clearly visible in the photographs which is the basis of proposed analysis method, see Fig. 2.

Photographs had to be prepared by dividing the video files into separate images, cropping and converting them into grayscale images. The amount of the frost was determined by counting the pixels representing frost in the photos using the algorithm available in NI Vision Builder 2013 as a part of NI LabView environment. Its operation was described below in a synthetic way.

In the first step the video files containing photographs of the tested cooler were converted into grayscale images. Next, the range of shades representing frost was chosen after carrying out a significant number of tests. Analysing several dozen hours of recordings, where pictures were taken every second, allowed to credibly verify the correctness of the operation of the proposed algorithm.

The inspection algorithm prepared in the Vision Builder (Fig. 3), consists of three steps: acquisition of photos, counting pixels and saving the results to a text file.

The second step (Count Pixels) adds up pixels in shades from previously chosen range. This option works only with grayscale images, this is why pictures had to be converted from RGB color model, in which they were taken by the camera.

The scope of shades included by the Count Pixels tool can be set manually or by several automatic routines. In this analysis authors used the Gray Objects option with manually adjusted thresholds of colors. The right selection of the range of shades is a key issue. It was chosen after a careful observation of the cooler photographs under various states of the frosting process. Ultimately a span of 90^{th} to 170^{th} shade was picked. The blue area visible in Fig. 4 are all pixels that fall into this range. The difference between a frosted and a clean cooler surface is clearly visible which is the basis of carried out analysis.

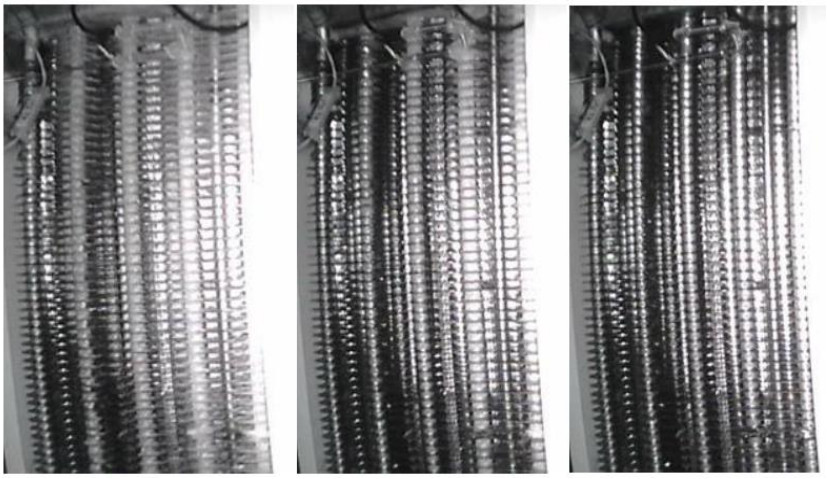

Figure 2: Photograph of the frosted cooler (left), between defrosting cycles (middle) and after the defrosting (right)

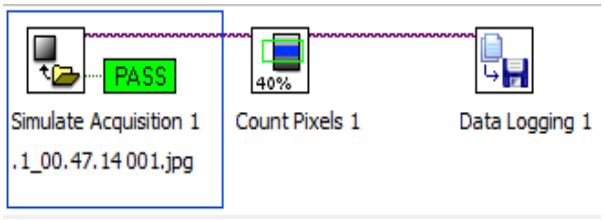

Figure 3: Inspection algorithm used to analyse the photographs

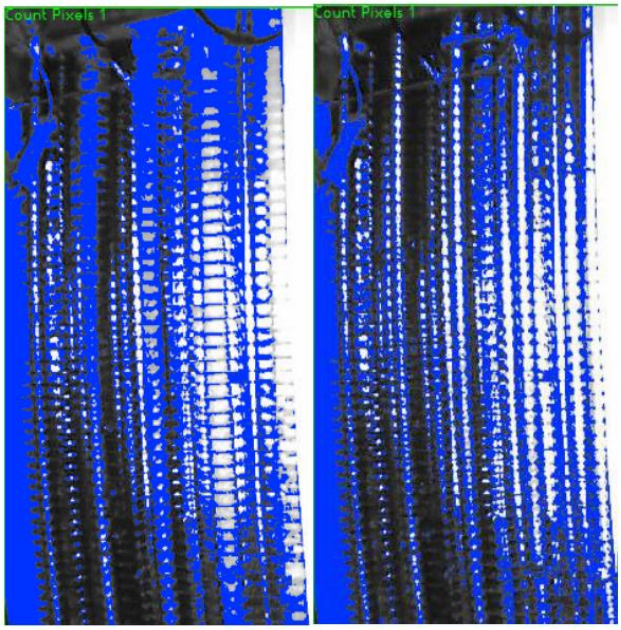

Figure 4: The air cooler pictures during analysis: before (left) and after defrosting (right)

The proposed method requires careful preparation of the measurement system and processing the data. Photographs must be of high quality, they must be synchronized with saved measurements, and correct selection of the colors range corresponding to the frost requires insightful observation and analysis of significant number of images.

3. RESULTS'

Four measurements series were analyzed. Additionally, to the comparison of selected measurements with the intensity of the frosting, the heat exchanger thermal capacity, thermal resistance and the bypass factor were calculated. All of the diagrams were plotted as a function of time with 24 hours on the horizontal axis. The data collected during the defrosting process were removed from the plots as most of the parameters, especially air and glycol temperatures, reach high values and reduced the readability of the diagrams.
The air cooler thermal capacity calculated for the glycol side, the bypass factor, and the change in thermal resistance after frosting were calculated according to the following formulas:

$$\dot{Q} = \dot{V}_g \rho_g c_g \left(t_{g\_out} - t_{g\_in} \right) \tag{1}$$

$$BF = \frac{t_2 - t_s}{t_1 - t_s} \tag{2}$$

$$\Delta R_{fr} = \frac{1}{k - k_{fr}} \tag{3}$$

The analyzed heat exchanger was being defrosted every 12 hours. Its surface did not frost evenly between defrosting cycles which is visible in Fig. 5. Sometimes after the defrosting process the amount of frost on the air cooler surface quickly rose to a higher level than before the defrosting conditions.
The percentage of the pixels representing frost in the pictures varied from about 32% to about 50%. For each measurements series the lowest percentage was subtracted from the percentage calculated for each photograph in a given series. This minimum has been accepted as a moment when the air cooler surface was completely clean. Additionally, the readability of the images was increased.
The percentages returned by NI Vision Builder only indicates the number of the pixels that fall into the chosen span of 90th to 170th shade of grey in the whole photograph. It is an indirect measure, proportional to the amount of ice on the air cooler surface. Zero percent in the graph (Fig. 5) describes the moment when the air cooler surface is clean. Also, 100% does not mean that cooler is completely frozen due to the presence of other elements in the picture.
The plots from the third measurements series were presented in the paper. In the first half of the series the course of the frosting is similar to other series (Fig. 5). The beginning of the plot depicts a stage after the second defrosting of the previous day. The air cooler gradually covers up with ice up to the first defrosting cycle at 8:00 am. After the ice has been removed, a quick frosting and a steady increase in the amount of frost up to the second defrosting occurred. The air temperature (Fig. 6) before the cooler increases slightly with frosting. Temperature behind the cooler changed inversely. These changes are small at the order of 0.1K. Temperatures of glycol (Fig. 7) decreased slightly with frosting process of the air cooler.

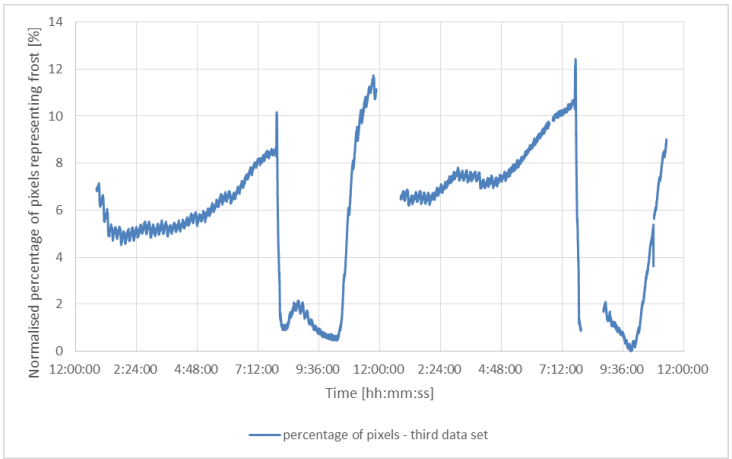

Figure 5: Amount of frost on the exchanger surface

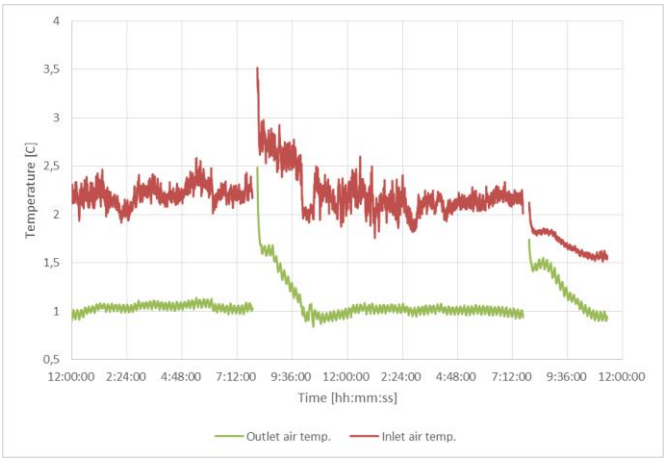

Figure 6: Air temperatures distributions

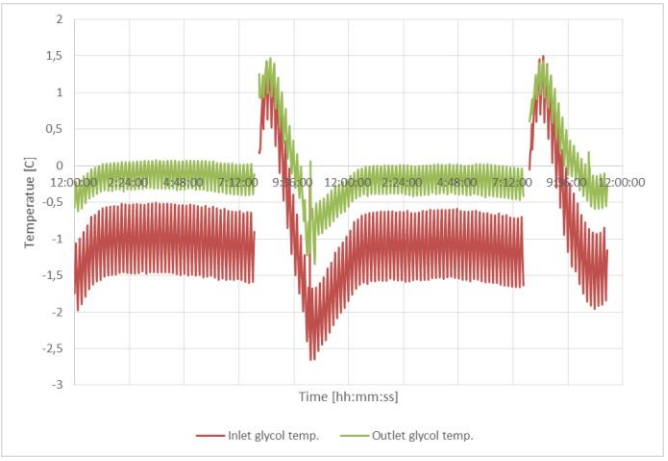

Figure 7: Glycol temperature distribution

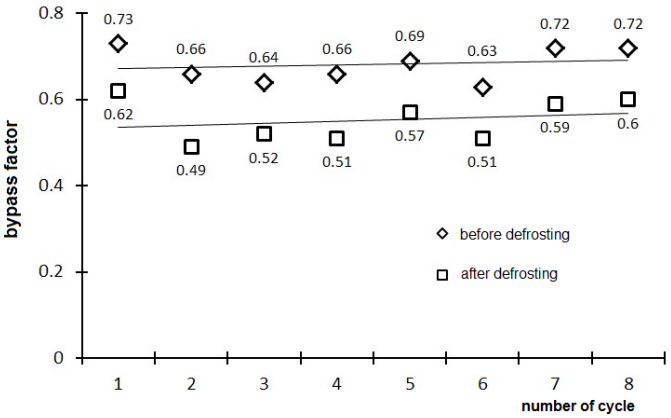

Figure 8: Bypass factor before and after defrosting in subsequent cycles

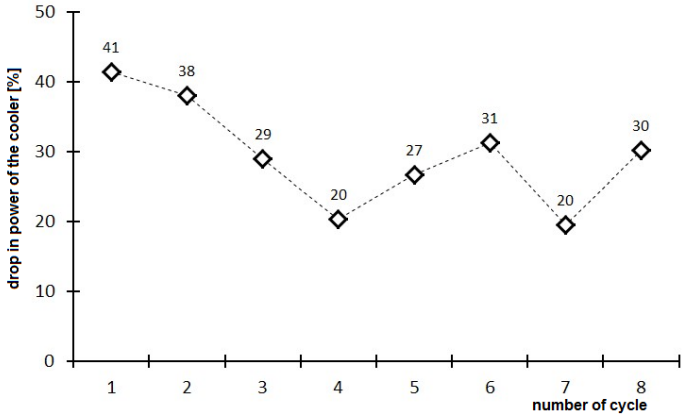

Figure 9: Drop in the air cooler thermal capacity under frost conditions in subsequent cycles

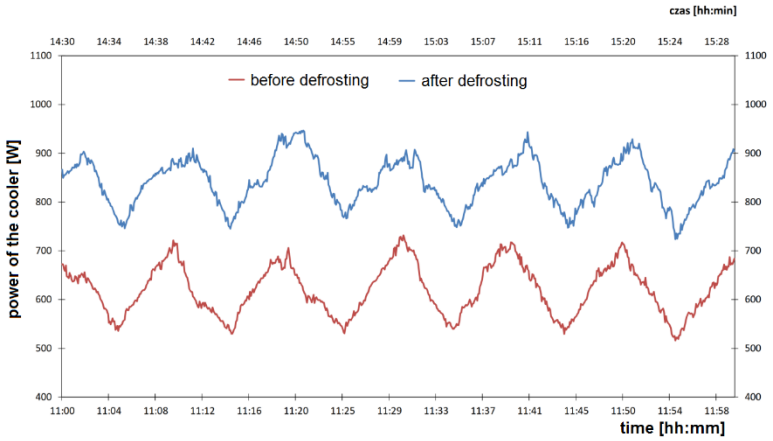

Figure 10: The air cooler thermal capacity calculated for the glycol side

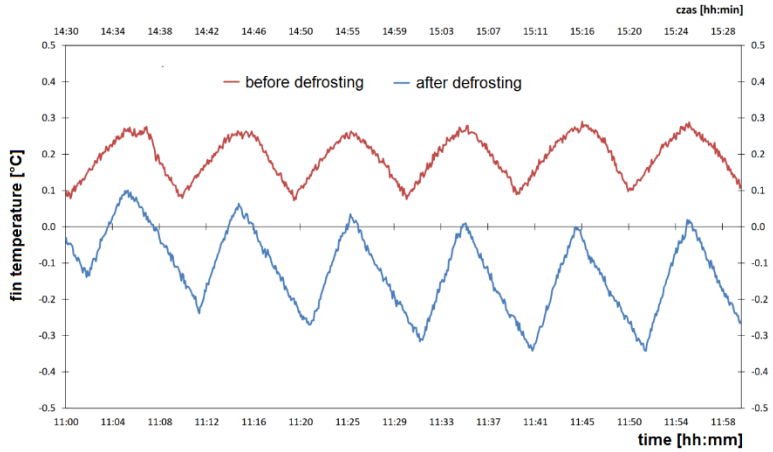

Figure 11: Fins temperatures distributions

Table 1: The performance parameters of the tested air cooler

Before defrosting			After defrosting			
$\dot{Q}_{c,fr}$ [W]	k_{fr} [W/(m^2 K)]	BF_{fr}	$\dot{Q}_{fr}$ [W]	k [W/(m^2 K)]	BF	ΔR_{fr} [m^2 K/W]
145.8	18	0.73	249.2	31	0.62	0.08
155.3	12	0.66	250.9	19	0.49	0.13
153.2	12	0.64	215.8	17	0.52	0.20
170.6	12	0.66	214.3	15	0.51	0.32
181.1	12	0.69	247.1	17	0.57	0.22
153.2	11	0.63	223.2	17	0.51	0.18
223.1	13	0.72	277.6	16	0.59	0.31
247.8	21	0.72	355.2	30	0.60	0.11

The power on the glycol side (Fig. 10) grows when the cooler is frosting up. Bypass factor (Fig. 8) calculated according to eq. (2) may be thought as very high and varied from 0.5 (clean heat exchange surface) up to 0.7 (frosted up surface). In the analyzed period the air cooler thermal capacity varied from 0.75 kW up to 0.90 kW. The lowest calculated thermal capacity was about 0.35 kW, and the highest one app. 1.20 kW

The results indicate that frosting process deteriorates the air cooler thermal capacity by 20 – 40% by increasing its bypass factor BF (Fig. 8 and Fig. 9) since it increases within the range 18 – 35%. The average bypass factor of the frosted cooler was 0.68 while it reaches 0.55 after the defrosting process. Maximum rise in thermal resistance was 0.32 m^2×K/W in the tested cases.

4. CONCLUSIONS

Proposed method of analysis allows to assess the extent of frosting process and its influence on the air cooler thermal performance. A correlation between the frosting plots (Fig. 5) and the measured parameters is clearly visible, especially in the case of air humidity, glycol and air temperatures and the air cooler thermal capacity. However, this way of the assessment of the air cooler frosting conditions requires the accurate preparation of the measurements and visualization material.

It is necessary to identify all of the measurements that are related to the frosting process. Fundamental parameter which have also been included in this paper are air and glycol temperature before and after the tested air cooler, temperature of the fins and flow rate of the cooling fluid.

The photographs of the air cooler surface are also essential. Well-prepared images facilitate the assessment of the amount of frost and increase the accuracy of the obtained results. All photos should be taken under the same conditions, i.e. with the same lighting and position of the camera. This allows using the same span of colors for all of the images. Other phenomena that might affect the results returned by the counting algorithm must also be taken into consideration, e.g. the change of the frost surface structure at the beginning of the defrosting process.

NOMENCLATURE

BF	bypass factor	(–)
c	specific heat	(kJ/kg K)
t	temperature	(°C)
$\dot{V}$	volumetric flow rate	(m^3/s)
ρ	density	(kg/m^3)

Subscript

c	cooler
fr	frost conditions
g	glycol
in	inlet of the cooler

out	outlet of the cooler
1	in front ofthe cooler
2	behind the cooler

REFERENCES

Chiwon, K., Jaehwan, L., Kwan-Soo, L. (2017). Numerical modeling of frost growth and densification on a cold plate using frost formation resistance, *International Journal of Heat and Mass Transfer 115*, Part A, 1055-1063
Song, M., Deng, S., Dang, C., Mao, N., Wang, Z. (2018). Review on improvement for air source heat pump units during frosting and defrosting, *Applied Energy 211*, 1150-1170
Reindl D.T., Jekel T.B. (2009). *Defrosting Industrial Refrigeration Evaporators*, ASHRAE Journal.
Xiaomin, W., Shan, H., Fuqiang, C. (2016) Experimental study of frost formation on cold surfaces with various fin layouts, *Applied Thermal Engineering* 95, 95-105.

ACKNOWLEDGEMENT

The research results presented in the paper were completed within the statutory activities S/WM/1/2018 and financed by Ministry of Science and Higher Education.